

The luminosities of backsplash galaxies in constrained simulations of the Local Group

Alexander Knebe¹, Noam I Libeskind², Steffen R. Knollmann¹, Luis A. Martinez-Vaquero¹, Gustavo Yepes¹, Stefan Gottlöber², Yehuda Hoffman³

¹*Grupo de Astrofísica, Departamento de Física Teórica, Modulo C-15, Universidad Autónoma de Madrid, Cantoblanco E-28049, Spain*

²*Astrophysikalisches Institut Potsdam, An der Sternwarte 16, D-14482 Potsdam, Germany*

³*Racah Institute of Physics, The Hebrew University of Jerusalem, Jerusalem 91904, Israel*

First draft

ABSTRACT

We study the differences and similarities in the luminosities of bound, infalling and the so-called backsplash (Gill et al. 2005) galaxies of the Milky Way and M31 using a hydrodynamical simulation performed within the Constrained Local UniversE Simulation (CLUES) project. The simulation models the formation of the Local Group within a self-consistent cosmological framework. We find that even though backsplash galaxies passed through the virial radius of their host halo and hence may have lost a (significant) fraction of their mass, their stellar populations are hardly affected. This leaves us with comparable luminosity functions for infalling and backsplash galaxies and hence little hope to decipher their past (and different) formation and evolutionary histories by luminosity measurements alone. Nevertheless, due to the tidal stripping of dark matter we find that the mass-to-light ratios have changed when comparing the various populations against each other: they are highest for the infalling galaxies and lowest for the bound satellites with the backsplash galaxies in-between.

Key words: methods: n-body simulations – methods: numerical – galaxies: formation – galaxies: haloes

1 INTRODUCTION

Ever since Klypin et al. (1999) and Moore et al. (1999) pointed out that dark matter simulations of cosmic structure formation lead to an excess of subhaloes as compared to the number of observed (luminous) satellite galaxies visibly surrounding the Milky Way (MW) and M31, the industry for simulating and studying substructure in cosmological (dark matter) haloes has boomed. The tension has been marginally loosened with the discovery of a substantial number of new ultra-faint satellites galaxies in the Local Group thanks to the SDSS data (Adelman-McCarthy 2007): within the past couple of years the number of known MW and M31 satellites has nearly doubled. And taking into account the detection limits and the sky coverage of the SDSS survey we will most certainly stumble across even more galactic satellites in the near future when, for instance, upcoming data from GAIA and panSTARRS have been analysed.

As noted by several groups before (Moore et al. 2004; Gill et al. 2005), there exists a prominent population of galaxies that are found outside the virial region of their host at the present day, but whose orbits took them inside the virial radius at earlier times. While their studies were based upon cosmological simulations of galaxy clusters, the existence of this “backsplash population” has also been found for MW-type objects (Warnick et al. 2008; Ludlow et al. 2009). This raises the question whether or not

(and how) one can distinguish infalling and backsplash galaxies from each other. Gill et al. (2005) suggested to use the line-of-sight velocity distribution: as shown in their Fig.8 the distribution of line-of-sight velocities of subhaloes relative to the host (and convolved with the 2dF velocity uncertainty of 100 km/sec) is different for the infalling and the backsplash population. However, there may be a simpler way that does not involve spectroscopy. Since backsplash satellites had, at one point in their orbit, a closer approach to the central galaxy than infalling satellites, the tidal influence of the host must have been stronger for the backsplash population than for infalling satellites. Could this difference in tidal forces effect the initial stellar population (if existent), and can it be used to discriminate between the two populations? It has been shown by Gill et al. (2005) that backsplash galaxies loose on average 40% of their initial mass when grazing their host. But what about the stellar content? As baryons are able to cluster more strongly in the centre of the potential well the stars are also more centrally concentrated. Therefore, will the cold baryonic component be safe from tidal stripping when the backsplash galaxy (briefly) flies through its host? This question is the major motivation for this work. We address the issue of separating the three types of galaxies (bound satellites, backsplash and infalling) by means of luminosity (and possibly mass) measurements only.

2 THE SIMULATIONS

In this Section we describe the simulations used throughout this study and the methodology employed to identify host haloes and their substructure.

2.1 Constrained Simulations of the Local Group

We use the same set of simulations already presented in Libeskind et al. (2010) and Knebe et al. (2010) and refer the reader to these papers for a more exhaustive discussion and presentation of these constrained simulations of the Local Group that form part of the CLUES project.¹ However, we briefly summarize their main properties here for clarity.

We choose to run our simulations using standard Λ CDM initial conditions, that assume a WMAP3 cosmology (Spergel et al. 2007), i.e. $\Omega_m = 0.24$, $\Omega_b = 0.042$, $\Omega_\Lambda = 0.76$. We use a normalization of $\sigma_8 = 0.73$ and a $n = 0.95$ slope of the power spectrum. We used the PMTree-SPH MPI code GADGET2 (Springel 2005) to simulate the evolution of a cosmological box with side length of $L_{\text{box}} = 64h^{-1}\text{Mpc}$. Within this box we identified (in a lower-resolution run utilizing 1024^3 particles) the position of a model local group that closely resembles the real Local Group (cf. Libeskind et al. 2010). This Local Group has then been re-sampled with 64 times higher mass resolution in a region of $2h^{-1}\text{Mpc}$ about its centre giving a nominal resolution equivalent to 4096^3 particles giving a mass resolution of $m_{\text{DM}} = 2.1 \times 10^5 h^{-1}M_\odot$ for the dark matter and $m_{\text{gas}} = 4.42 \times 10^4 h^{-1}M_\odot$ for the gas particles. For more details we refer to the reader to Gottlöber et al. (2010).

For this particular study we focus on the gas dynamical SPH simulation, in which we follow the feedback and star formation rules of Springel & Hernquist (2003): the interstellar medium (ISM) is modeled as a two phase medium composed of hot ambient gas and cold gas clouds in pressure equilibrium. The thermodynamic properties of the gas are computed in the presence of a uniform but evolving ultra-violet cosmic background generated from QSOs and AGNs and switched on at $z = 6$ (Haardt & Madau 1996). Cooling rates are calculated from a mixture of a primordial plasma composition. No metal dependent cooling is assumed, although the gas is metal enriched due to supernovae explosions. Molecular cooling below 10^4K is also ignored. Cold gas cloud formation by thermal instability, star formation, the evaporation of gas clouds, and the heating of ambient gas by supernova driven winds are assumed to all occur simultaneously.

2.2 The (Sub-)Halo Finding

In order to identify halos and subhaloes in our simulation we have run the MPI+OpenMP hybrid halo finder AHF² described in detail in Knollmann & Knebe (2009). AHF is an improvement of the MHF halo finder (Gill et al. 2004), which locates local over-densities in an adaptively smoothed density field as prospective halo centres. The local potential minima are computed for each of these density peaks and the gravitationally bound particles are determined. Only peaks with at least 20 bound particles are considered as haloes and retained for further analysis (even though we place a tighter constraint on the number of particles for the present analysis, cf. below). We like to stress that our halo finding algorithm automatically

identifies haloes, sub-haloes, sub-subhaloes, etc. For more details on the mode of operation and actual functionality we though refer the reader to the code description paper by Knollmann & Knebe (2009).

Subhaloes are defined as haloes which lie within the virial region of a more massive halo, the so-called host halo. We build merger trees by cross-correlating haloes in consecutive simulation outputs. For this purpose, we use a tool that comes with the AHF package called MergerTree, that follows each halo (either host or subhalo) identified at redshift $z = 0$ backwards in time. The direct progenitor at the previous redshift is the object that shares the most particles with the present halo *and* is closest to it in mass. Again, for more elaborate details we point to the reader to Libeskind et al. (2010).

2.3 Lighting up Subhaloes

The stellar population synthesis model STARDUST (see Devriendt et al. 1999, and references therein for a detailed description) has been used to derive luminosities from the stars formed in our simulation. This model computes the spectral energy distribution from the far-UV to the radio, for an instantaneous starburst of a given mass, age and metallicity. The stellar contribution to the total flux is calculated assuming a Kennicutt initial mass function (Kennicutt 1998).

3 RESULTS

The prime target of this study is to find possible differences in the properties of backsplash, bound and infalling galaxies with respects to luminosity. We explicitly use the term “galaxies” as we focus solely on subhaloes with a luminous stellar component; all other objects will be neglected for this particular investigation. We further only consider satellites of the (simulated) MW and Andromeda (M31) galaxy; the subhaloes of both these host haloes will be stacked in the subsequent plots presented here. In addition to the requirement for subhaloes to contain stars we also apply a lower mass cut of $M > 2 \times 10^7 h^{-1}M_\odot$ roughly corresponding to 100 particles in total (note that particles have different masses as they represent dark matter, gas and stars).

3.1 The Existence of Backsplash Galaxies

Before examining the properties of backsplash galaxies we wish to first confirm their existence. To this extent we plot in Fig.1 the closest approach (normalized to the virial radius of the satellite’s host at the time of minimum distance) vs. its present-day distance (normalized to its host’s virial radius). The number of objects in the respective population are given in the legend. Note that we only plot those subhaloes that contain a stellar component. This figure contains three distinct parts defining the three different populations. First, those subhaloes whose minimum distance equals its present-day distance are the infalling population: they are continuously falling towards their host. Second, galaxies that entered the virial radius of their host and remained inside ever since. Even though the host radius is increasing in size since the time a subhalo entered, we nevertheless find that there are no subhaloes above the 1:1 line; we therefore conclude that the increase in host radius as measured by $R_{\text{host}}^{\text{now}}/R_{\text{host}}^{\text{min}}$ is smaller than the ratio $D_{\text{now}}/D_{\text{min}}$. This comes as no surprise as we do not expect satellites to orbit on circular orbits ($D_{\text{now}} = D_{\text{min}}$); subhaloes may have (highly) eccentric

¹ <http://www.clues-project.org>

² AMIGA halo finder, to be downloaded freely from <http://www.popia.ft.uam.es/AMIGA>

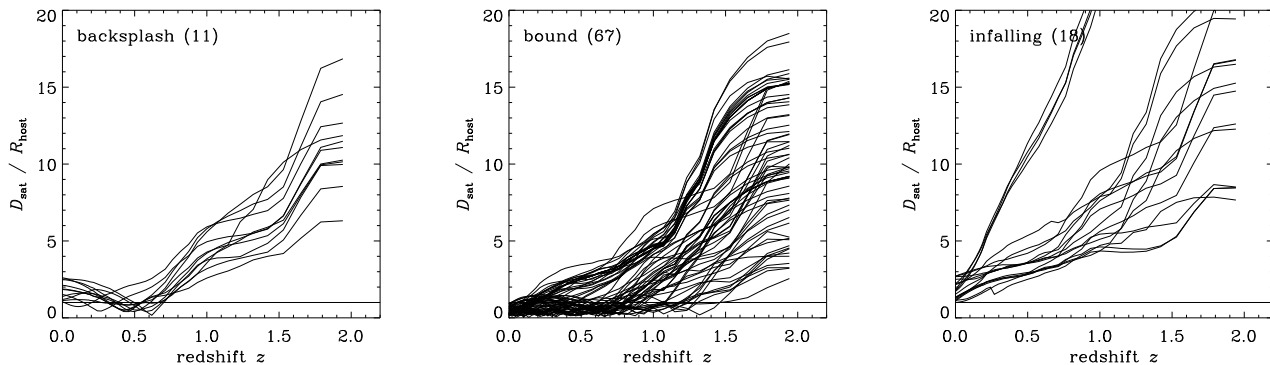


Figure 2. The orbits of all considered subhaloes. The left panel shows the backsplash galaxies, the middle panel the bound and the right panel the infalling population.

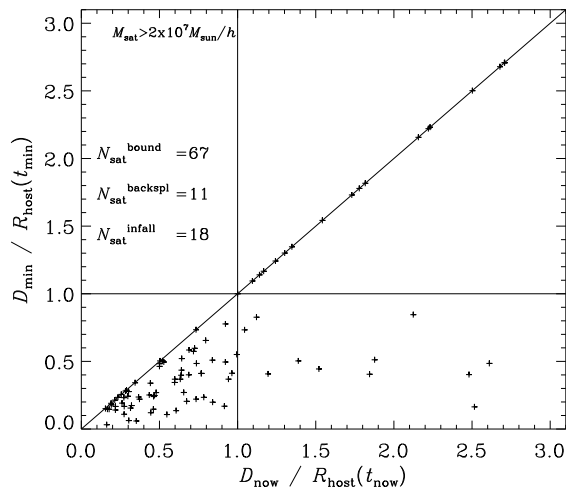


Figure 1. Minimum distance D_{\min} as a function of present-day distance D_{now} both normalized to the virial radius of the host at the respective time.

orbits taking them close to the centre of their host (cf. Figs. 7 and 8 in Gill et al. 2004). Third and last, there are galaxies that once were inside their host’s virial radius but are presently found outside, i.e. the backsplash population.

Fig. 1 indicates that we might expect to find of order 40% to be backsplash galaxies in the vicinity of the Milky Way and/or M31 – a percentage in agreement with previous studies of this class of objects (cf. Gill et al. 2005; Warnick et al. 2008). The question now is whether or not we will be able to distinguish these populations and find the backsplash galaxies, respectively, by quantifying their luminosities.

Before proceeding we would like to add a cautionary remark clarifying our terminology: we call subhaloes that are inside their host’s virial at $z = 0$, “bound”. Those subhaloes that were once inside their hosts virial radius but are found at $z = 0$ outside are termed “backsplash”. As we can see from Fig. 2 this classification strongly depends on the redshift used to define the populations. We can see that a fair fraction of today’s bound population had been backspashed in the past, while probably all of today’s backsplash galaxies will return and re-enter their hosts at some future time. Therefore, the expression “bound” should not be taken literally (in

terms of energy arguments) but rather as a reference to satellites under a prolonged influence of their host while “backsplash” refers to satellites under brief influence of their host. Further, please note that we require objects to exist both at redshift $z = 1.5$ and today to be part of our sample; there are also subhaloes that were present at high redshift but got tidally disrupted and hence did not survive.

In preparation of the investigation the luminosities in Section 3.2 and baryon content in Section 3.3, we wish to find the time where all three populations were still infalling so as to verify the correctness of our tracking scheme for subhaloes. To this extent we present in Fig. 2 the distance from the center of their hosts of all backsplash (left panel), bound (middle panel), and infalling (right panel) galaxies found and identified at redshift $z = 0$. The orbits have been normalized to the virial radius of the respective host (at redshift z) of each galaxy and hence the solid line $D_{\text{sat}}/R_{\text{host}} = 1$ marks the “entry” (and “exit”) point of the satellite into and out of the host. While this figure succinctly demonstrates that backsplash galaxies clearly entered and exited their host (while infalling galaxies have not yet crossed the virial radius) it also allows us to find that point in time in our simulation at which *all* populations were still infalling: this can be seen at a redshift $z \geq 1.5$. We will return to this redshift later as we expect the properties of galaxies to be drawn from the same statistical distribution at that time: no galaxy has yet entered the host (or left again) which may (or may not) have caused changes in the internal properties and – in particular – the luminosities.

3.2 The Luminosities

In this section we look at the luminosity of the stellar components of galaxies identified as bound, backsplash and infalling. We start by comparing, in Fig. 3, the Johnson V-Band luminosity of the bound satellites to the backsplash and infalling population of galaxies as well as the observational data as taken from Koposov et al. (2008) and Macciò et al. (2010), respectively (thin solid line, referred to as “Maccio’ sample” from now on); these data are a combination of the volume corrected MW satellite luminosity function (Koposov et al. 2008) augmented with information from Mateo (1998) and Macciò et al. (2010) kindly provided to us by Andrea Maccio (personal communication). And even though our bound luminosity function agrees with the Maccio data rather well, we stress that we included the observational data merely as a reference to guide the eye. It is not our prime objective to repro-

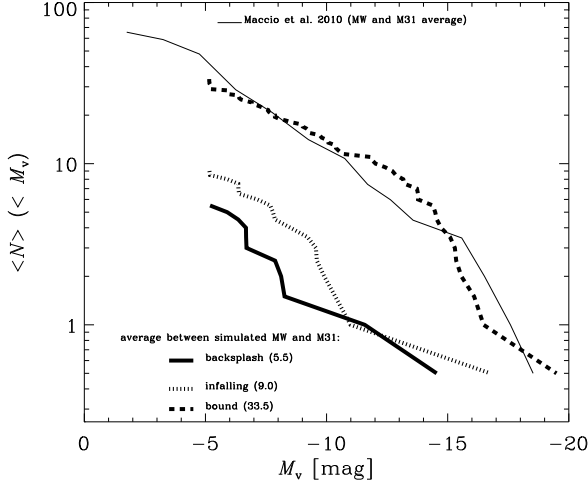


Figure 3. The luminosity function of subhaloes in the Johnson V-Band. The “Maccio” observational data (thin solid line) is a combination of the volume corrected MW luminosity function Koposov et al. (2008) augmented with information from Mateo (1998) and Macciò et al. (2010) under the assumption of an NFW-like radial distributions of satellites. Note that the comparison to the observational data is *not* the prime target of this study and only serves as a reference, respectively.

comparison			p
$z = 0$			
bound	–	backplash	0.114
bound	–	infalling	0.190
backplash	–	infalling	0.667
$z = 1.5$			
bound	–	backplash	0.051
bound	–	infalling	0.443
backplash	–	infalling	0.417

Table 1. Kolmogorov-Smirnoff (KS) probabilities p for various comparisons of the luminosity functions presented in Fig.3.

duce the MW and/or M31 luminosity function of satellite galaxies with our simulation. However, a close match (as seen in Fig.3) reassures us that our simulation is not too far fetched and that our method for lighting up subhaloes (cf. Section 2.3) yields credible results. The central theme of this paper is the comparison between the (numerically obtained) infalling and backplash population and possibilities to decipher them photometrically.

To better quantify the differences and similarities between the respective simulated luminosity functions we applied the Kolmogorov-Smirnoff (KS) test that provides us with the significance level p that the null hypothesis that two data sets are drawn from the same parent distribution; small values of $p \in [0, 1]$ show that the two cumulative distribution functions (i.e. in our case two luminosity functions) are significantly different.³ We find that the KS probability that the backplash and infalling distributions have been drawn from the same parent function is 67%. The significance

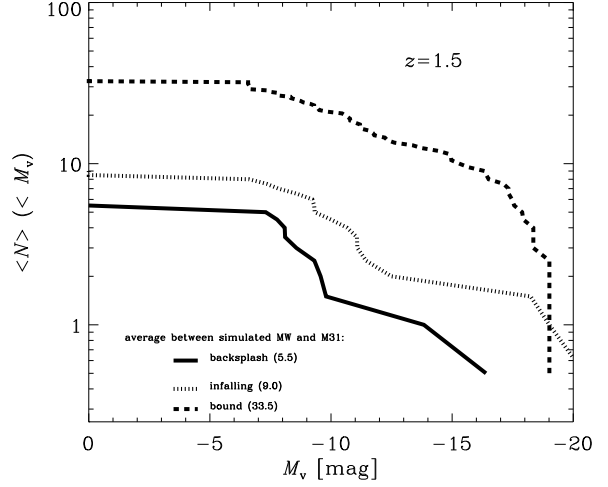


Figure 4. The luminosity function of subhaloes in the Johnson V-Band at redshift $z = 1.5$ (i.e. the redshift at which none of the galaxies has yet entered their respective host).

level is just 11% when comparing the backplash with the bound population and 19% when comparing the infalling with the bound satellites. These numbers and probabilities, respectively, have been summarized in Table 1.

In addition to calculating the KS probability p that these distributions stem from the same parent distribution we also performed the experiment of randomly drawing N_{back} galaxies from the infalling and bound sample where N_{back} is the number of backplash galaxies. Comparing the resulting down-sampled luminosity functions again using a KS test we find a probability p of $p \approx 0.66$ when comparing the backplash population to the infalling one and $p \approx 0.12$ when comparing the backplash to the infalling or bound satellites population. All this hints at similarities between backplash and infalling satellites whereas the bound population has likely evolved differently.

Since all bound and backplash galaxies themselves were, at some stage, infalling satellites the differences between the bound and backplash/infalling luminosity function at redshift $z = 0$ should (at least) be lessened when moving to a time where none of the objects had entered their host, i.e. redshift $z = 1.5$ (cf. Fig.2 in Section 3.1); the three (cumulative) distributions of luminosities at redshift $z = 1.5$ are presented in Fig.4. Performing the same exercises of comparing the various distributions using the KS statistic (cf. Table 1 again), we obtain a marginally larger probability for the infalling population to agree with the bound and backplash subhaloes. However, the compatibility between the bound and backplash is actually lowered. In that regards we need to stress that the number of satellites – despite combining MW and M31 – is not very large (especially not for the backplash population) and hence any (extensive) statistical analysis has to be taken with care. Therefore, the probabilities presented here are more indicative of possible trends rather than providing hard evidence for similarities and/or differences.

Even though our primary motivation is to find a way to distinguish backplash from infalling satellites that only utilizes photometry, we nevertheless present another (observable) correlation: the luminosity vs. the velocity dispersion σ_v , in Fig.5. As already alluded to above when discussing the luminosity function, we also

³ We utilized the routine `kstwo()` as described in Press et al. (1992).

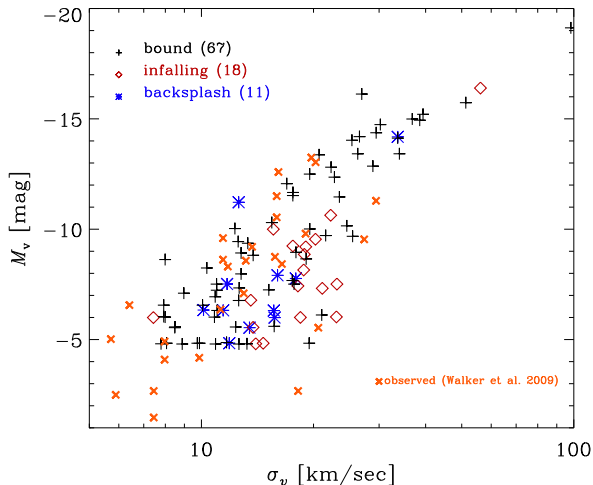


Figure 5. The relation between Johnson V-Band luminosity and subhalo velocity dispersion at redshift $z = 0$. The observational data is taken from Walker et al. (2009).

added observational data (taken from Walker et al. (2009, their Table 1)) simply to guide the eye. While we also recover the observed trend in our numerical data, the focus should lie with the infalling and backplash galaxies. To better quantify the correlations between σ_v and M_V we calculated the Spearman rank coefficients R_S :⁴ for the observational data it amounts to $R_S = 0.687$ whereas there appears to be a marginally stronger correlation for our bound satellites of $R_S = 0.824$. However, this “discrepancy” is likely due to the different magnitude limits of both the observational and numerical data, i.e. the two data sets do only cover the same magnitudes in the range $M_V \in [-13, -5]$.

The respective correlation coefficients R_S for the backplash and infalling populations are $R_S = 0.373$ and $R_S = 0.573$ respectively. While there are differences in the strengths of the correlation we find it difficult to utilize this interdependence to separate backplash from infalling satellites: while the Spearman rank significances S_S are very close to zero for the bound and observational data (indicating a reliable determination of the respective R_S value) they are of order 0.2 for the backplash and infalling population, probably due to the small statistical sample.

Above, we showed that while all three populations do follow the same trend for the $M_V - \sigma_v$ relation (coinciding with the trend found in observational data), there are nevertheless subtle differences in the strength of this correlation, especially for the backplash and infalling population (cf. the different Spearman rank coefficients R_S). However, the most prominent and well pronounced difference can be found when studying the mass-to-light ratios M/L_V presented in Fig. 6 as a function of V-band magnitude M_V . We stress that the mass M used in this plot is actually the mass within the visible radius of the subhalo; we found the distance of the

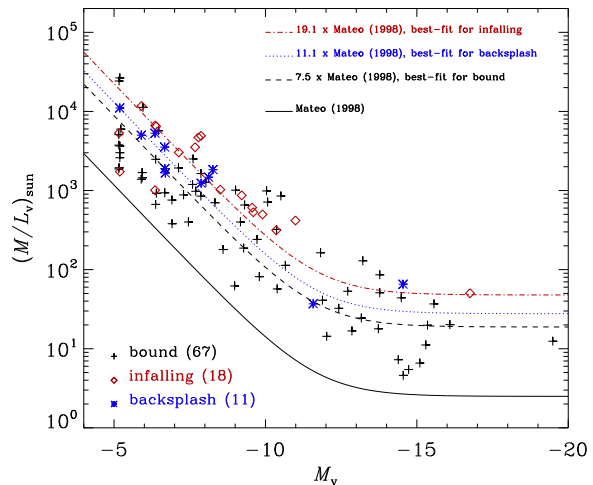


Figure 6. Mass-to-light ratios (in terms of solar values) as a function of V-band luminosity M_V . The thin solid line represents the observational relation as found by Mateo (1998). The other lines are the best-fit curves (with the amplitude as a free parameter) to the bound (dashed), backplash (dotted), and infalling (dot-dashed) population, respectively, with the legend listing the respective value of the amplitude, too. Note that we used the “mass M inside the visible radius” as described in the text for this plot.

farthest stellar particle and used the total mass interior to this radius as M . Wadepuhl & Springel (2010) already noted that a (substantial) shift (i.e. $A \approx 5.2$) of the observationally determined analytical relation

$$\frac{M/L}{(M/L)_\odot} = A \left(2.5 + \frac{10^7}{L/L_\odot} \right) \quad (1)$$

is required (Mateo 1998, $A = 1$ in there), which is confirmed by our data: leaving A as a free parameter and using only the bound, backplash, and infalling satellites we find $A = 7.5 \pm 0.7$ (bound), $A = 11.1 \pm 1.2$ (backplash), and $A = 19.1 \pm 2.4$ (infalling).⁵ These different amplitudes are naturally explained by the differing histories and (strengths of) interactions with the host. We will see below in Section 3.3 that bound galaxies lost the largest amount of their dark matter when compared with the other two populations; infalling satellites are in fact still gaining mass through accretion. Therefore, taken together with the fact that their luminosities are nevertheless still similar, we may infer that the mass-to-light ratios should be significantly different. This notion opens up the possibility to use the relation presented in Fig. 6 to separate the three populations from each other. In practice this requires not only photometric measurements but also a (proxy for the) mass estimation.

However, using the mass inside the stellar radius also may explain the differences found in Fig. 6: stars in real satellites may be more compact relative to the dark matter than in our simulation, and might therefore be less susceptible to tidal stripping (together with the dark matter inside the “visible” radius). This would also suggest that the differences between our three different populations might be smaller if the luminous parts of the satellites were more compact.

⁴ The Spearman rank coefficient R_S is a non-parametric measure of correlation: it assesses how well an arbitrary monotonic function describes the relationship between two variables, without making any other assumptions about the particular nature of the relationship between the variables (Kendall & Gibbons 1990). Its significance S_S is a value between 0 and 1 and a small value indicates a significant correlation. We use the IDL routine `R.CORRELATE()` to calculate both these numbers.

⁵ The fitting to Eq.(1), i.e. a function $M/L(L)$, has been done using IDL’s `CURVEFIT` routine using equal weights for the data points M/L vs. M_V ; the reported standard deviations had been returned by `CURVEFIT`, too.

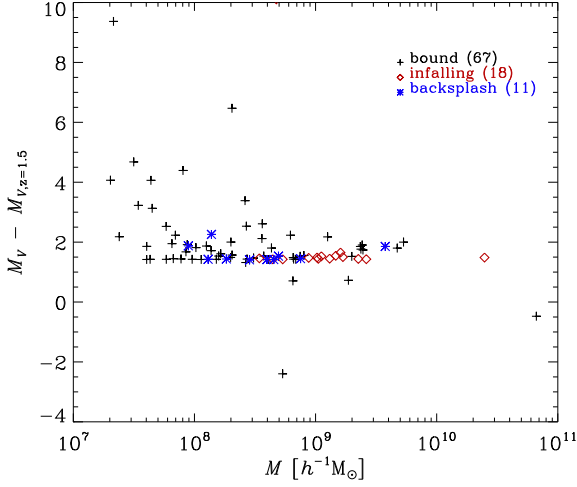


Figure 7. Difference between Johnson V-Band luminosity at present day and redshift $z = 1.5$ as a function of present day halo mass M .

We further like to mention that we not only used the mass inside the stellar radius as a measure for the mass entering the mass-to-light ratio. We also applied various other definitions, e.g. the total mass inside the virial radius as well as the mass as determined from the velocity dispersion under the assumption of virialisation and an NFW density profile (both at the virial radius and at 15% of the virial radius). While the amplitudes A are certainly different when using different mass estimates, the general trend remains unaltered: the M/L ratios for the infalling satellites are shifted upwards with respects to the backplash population which itself has higher ratios than the bound subhaloes.

However, we also need to bear in mind one of the subtleties of halo finding, especially subhalo finding: the definition of mass and the edge of a subhalo, respectively. While it is straight forward to define an outer edge for an (isolated) field halo (usually defined as the radius at which the mean interior density drops below 200 times the critical density), the situation is more tricky for subhaloes: they have to be truncated at the point where their density profile starts to rise again due to the host’s background density. Therefore, the same subhalo placed inside and outside of a host will have different masses due to the nature of (our) halo finding technique. This explains at least in part the offset in the mass-to-light ratios for bound/backplash and infalling galaxies: the infalling ones have in general higher masses. And part of the gap between bound and backplash may be explained by the same phenomenon, though not all of it; there certainly is no uncertainty that bound galaxies have lost more mass than backplash subhaloes.

The differences between the luminosities of the populations at redshift $z = 0$ and the (marginally) more pronounced similarities at a time where all populations were still infalling (i.e. redshift $z = 1.5$) calls for a closer look at the evolution of satellite galaxy luminosity. To this extent we plot in Fig.7 the difference between the Johnson V-Band luminosity M_V at redshift $z = 0$ and at redshift $z = 1.5$ as a function of the total bound halo mass M for each galaxy considered in this paper, using different symbols for the different populations (stars for backplash, plus-signs for bound, and diamonds for infalling galaxies).

Fig.7 now shows several things. For a substantial number of satellites (especially the backplash and infalling population) we

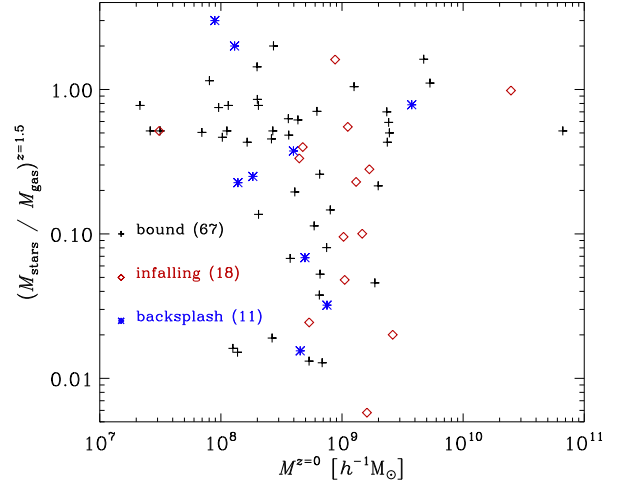


Figure 8. Ratio of stellar to gas mass at redshift $z = 1.5$ as a function of present day halo mass M .

only observe a “constant” decrease in luminosity of approx. 1.5 magnitudes. However, the luminosity of the bound galaxies drops significantly – especially on the low-mass end – while some of the higher mass ones gain luminosity. As luminosity is directly linked to stellar content we are left with the question of how these differences relate to changes in the stellar population and/or removal (or gain) of star particles from a subhalo. We study these issues in the following subsection.

Studying luminosities is also closely related to colours, i.e. ratios of luminosities in different wave-bands. It therefore appears natural to ask the question - and use the data available to us - to have a closer look at differences in colours for our three populations. When plotting the $B - V$ colour as a function of halo mass M (not presented here) we observe that there are practically no differences at all amongst the various subhaloes and populations, respectively. Neither is there a correlation with mass. Colour appears unaffected when categorizing galaxies as bound, infalling or backplash.

3.3 The Baryon Content

Before investigating the stellar component directly we would like to start with a few words on the subhalo gas content. We find that hardly any of the subhaloes under consideration contain a significant gas content at redshift $z = 0$. When expressed in terms of the cosmic baryon fraction the amount of mass in gas is of order $< 10^{-4}$ for more than 90% of the subhaloes. However, their stellar mass fractions (again in terms of the cosmic baryon fraction) is $> 10^{-4}$ for all of them (which is a direct outcome of restricting ourselves to a sample of subhaloes that contain a stellar component). The situation though is rather different at redshift $z = 1.5$ where we find that all of the progenitors of the subhaloes not only contained gas but the fraction of mass in gas is on average a factor two higher than that in stars which can be verified in Fig.8. Note that in this figure we plot the present day mass on the x -axis and the ratio of stellar-to-gas mass at redshift $z = 1.5$ on the y -axis. The fact that none of the gas is left at redshift $z = 0$ indicates that either the gas has been converted into stars through the process of star formation, or the gas has been stripped/removed through interactions with the

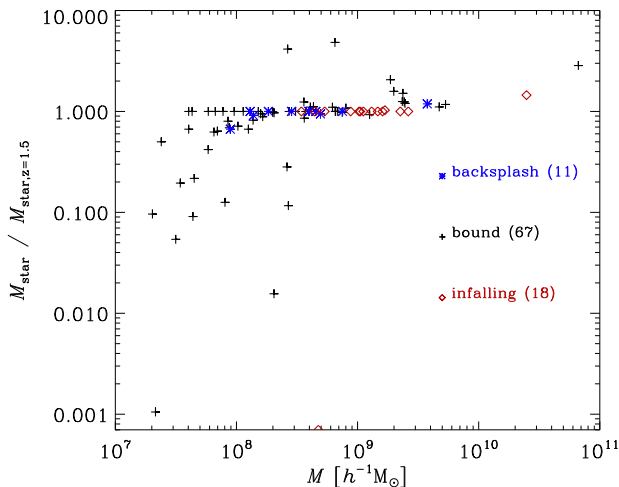


Figure 9. Ratio of stellar mass at present day and redshift $z = 1.5$ as a function of present day halo mass M .

host halo (e.g. ram pressure stripping) or other influences prior to infall. If the former is true we would expect to observe an increase in stellar mass since redshift $z = 1.5$, unless there is a conspiracy at work: the existing stars may be stripped at the same rate as star formation may convert gas into new stars, leaving the number of stars unchanged. However, this scenario is rather unlikely. We have also checked for the influence of the cosmological UV background: recall that in our simulations the thermodynamic properties of the gas are computed in the presence of a uniform but evolving UV cosmic background generated from quasi-stellar objects and active galactic nuclei and switched on at $z = 6$ (Haardt & Madau 1996). This prescription leads to an evaporation of gas in objects below a certain mass threshold $M_c(z)$ as given by Eq. (6) in Hoeft et al. (2006). When plotting the mass accretion histories of all our subhaloes under investigation here and comparing it to the aforementioned formula in Hoeft et al. (2006), we find that all the backsplash and infalling galaxies are in fact below the evaporation limit. For the bound objects we find that 1/3 are, at redshift $z = 1.5$, above that mass limit. However, they also drop below it by $z = 0$ (with the odd one remaining above). We therefore conclude that we should not be surprised to be left with subhaloes that contain hardly any gas at $z = 0$, due to photo-evaporation by the UV background.

The question now is, whether or not we find an evolution of the stellar component between redshifts $z = 1.5$ and $z = 0$. We therefore plot the ratio of the stellar content at these redshifts as a function of (present-day) subhalo mass in Fig.9. We observe that the backsplash (as well as the infalling) subhaloes hardly lost any stars since $z = 1.5$. Note that our simulations do not model stellar mass loss and hence the stellar mass remains constant when no star particles are stripped or newly created. However, this is still in agreement with the evolution of the luminosity as found in Fig.7: subhaloes with a constant number of stellar particles merely evolve passively from $z = 1.5$ to $z = 0$ due to stellar ageing. Nevertheless, the lower-mass subhaloes of the bound population did loose a substantial amount of stars while some of the higher-mass ones gained (or formed) stars. Therefore, a picture is now emerging, that while gas has been efficiently stripped, the stellar component remained more or less unaffected – at least for the infalling and backsplash population which are of prime interest in the present study.

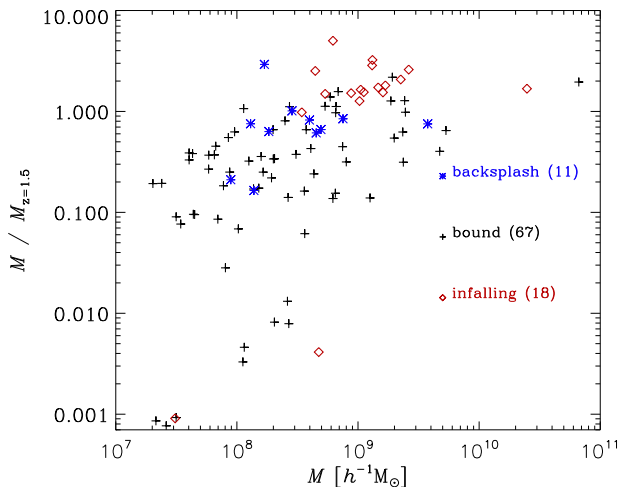


Figure 10. Ratio of total bound mass at present day and at redshift $z = 1.5$ as a function of present day halo mass M .

As we expect the stellar component to be concentrated at the centre of a subhalo, the previous finding on stellar mass loss for bound subhaloes immediately leads to questions regarding the nature of mass loss in general. To this extent we show in Fig.10 the ratio of total bound masses M (again as a function of today’s mass) at redshifts $z = 0$ and $z = 1.5$. We note that outside the influence of a host halo, subhaloes behave like field haloes and grow in mass through accretion processes; this is clearly confirmed for the infalling population (albeit with the exception of two objects). We also observe mass loss via tidal stripping, especially for the bound subhaloes. And while backsplash galaxies may at times loose as much as 40% of their original mass (Gill et al. 2005) we also find the odd backsplash galaxy in our particular sample that gained mass. Nevertheless, the picture is more or less clear: even though backsplash galaxies loose mass, their stellar component remains unaffected. This is not the situation for bound galaxies that loose both dark matter and stars due to the tidal interactions with the host, as expected. The picture drawn here therefore naturally explains the differences in the (amplitude of the) M/L_V ratios even though for that particular study only the “mass inside the visible radius” has been considered: when using the total bound mass (not presented here) we recover the same relations amongst the different subhalo populations with the ratios in amplitude unchanged; however, the absolute value of the amplitudes is more than a factor two higher.

4 DISCUSSION AND CONCLUSIONS

In this study we set out to examine the differences of the luminosities of backsplash, bound, and infalling satellite galaxies in a constrained cosmological hydrodynamical simulation of the Local Group. Our prime question is: Is it possible to distinguish these different population by mere photometry? While we find marginal differences in the bound vs. backsplash/infalling galaxies, the two populations residing in the outskirts of the host halo appear to have strikingly similar properties in terms of luminosity. The time backsplash subhaloes spent under the influence of the host is therefore not long enough to affect the stellar component: they loose mass, but primarily dark matter and/or gas particles are stripped - the star

particles remain more or less unaffected by the host’s tidal field. Therefore, their luminosity function and luminosities in general remain akin to the infalling population.

Nevertheless, when allowing for not only photometric information but also adding “mass” to our analysis, we found that the mass-to-light ratios (as a function of magnitude) are significantly higher in infalling than in backplash galaxies, which are in turn both higher than for bound satellites. Fitting the observationally determined relation presented in Mateo (1998) for M/L_V vs. M_V by leaving the amplitude as a free parameter we find differences in the amplitude of a factor of 1.5 and 2.5 between backplash and bound and infalling and backplash galaxies, respectively. We note, however, that part of this shift can be explained by (our method of) halo finding and certain endemic limitations when comparing field and subhaloes. The radial extent of a subhalo has to be truncated due to the embedding within the host’s background and hence has a lower mass than in the case when the same subhalo is found in isolation (i.e. exterior to a host halo) even though we explicitly only considered the “mass inside the visible radius” for this particular part of the investigation. We also need to acknowledge that the original relation had to be shifted by a factor of 7.2 to bring it into agreement with our numerical data⁶ which nevertheless is not the prime target of the present paper and its explanation left to a future study, respectively.

Even though there still remains a lot to be quantified, we believe that this difference may provide a new window on distinguishing between infalling and backplash galaxies that could be applied to observational data. Its origin is readily explained by the fact that while backplash and bound galaxies both lose mass the mass loss is greater for bound than for backplash galaxies; therefore, if the stellar population is unaffected (as found in our simulations) we observe an enhanced decrease in the mass-to-light ratios for bound galaxies and – more importantly for our purposes – a decrease when comparing infalling against backplash.

However, the apparent discrepancy between the simulation presented and used here and the observational data yet remains unexplained. It could be possible that stars in real satellites are more compact relative to the dark matter than in our simulation, and might therefore be less susceptible to tidal stripping (together with the dark matter inside the “visible” radius). But this would also suggest that the differences between our three different populations might be smaller if the luminous parts of the satellites were more compact closing the aforementioned “window” again. In that regards, we remind the reader that we not only used the mass inside the stellar radius as a measure for the mass entering the mass-to-light ratio. We also applied various other possibilities, e.g. the total mass inside the virial radius as well as the mass as determined from the velocity dispersion under the assumption of virialisation and an NFW density profile (both at the virial radius and at 15% of the virial radius). While the ratios of the M/L curves are certainly different when using different mass estimates, the forced trend remained unaltered.

A closer inspection of Fig.2 reveals that most of the backplash galaxies fell into their host at approximately the same time. When studying the distribution of infall times (not shown here though) there appears to be a continuous infall of bound galaxies whereas the backplash objects all cluster at about redshift $z \approx 0.55$. As pointed out by several other authors recently, subhaloes

may have the tendency to fall into (Milky Way like) hosts in groups (cf. Klimontowski et al. 2010; Li & Helmi 2009; D’Onghia & Lake 2008; Li & Helmi 2008). Hence could it be that all our backplash galaxies are part of a larger group? We explicitly checked for this conjecture by studying their 3D orbits and cannot confirm it: our backplash galaxies come from various directions yet fall in at a similar redshift. However, we also need to acknowledge that these directions are not random but rather correlated – however, this has been studied in detail in a companion paper Libeskind et al. (2010).

ACKNOWLEDGEMENTS

AK is supported by the Ministerio de Ciencia e Innovacion (MICINN) in Spain through the Ramon y Cajal programme and further acknowledges support by the Ministerio de Education (MEC) grant AYA 2009-13875-C03-02. SRK acknowledges support by the MICINN too under the Consolider-Ingenio, SyeC project CSD-2007-00050. We thank DEISA for granting us supercomputing time on MareNostrum at BSC and in SGI- Altix 4700 at LRZ, to run these simulations under the DECI- SIMU-LU and SIMUGAL-LU projects. We acknowledge support of MICINN through the Consolider-Ingenio 2010 Programme under grant MULTIDARK CSD2009-00064. We also thank ASTROSIM for giving us different travel grants to visit our respective institutions. GY acknowledges financial support from MEC (Spain) under project AYA 2009-13875-C03-02 and the ASTROMADRID project financed by Comunidad de Madrid. We thank Andrea Maccio for kindly providing us with the data of the observed luminosity function (average of MW and M31).

REFERENCES

- Adelman-McCarthy J. K. e. a., 2007, *ApJS*, 172, 634
- Devriendt J. E. G., Guiderdoni B., Sadat R., 1999, *A&A*, 350, 381
- D’Onghia E., Lake G., 2008, *ApJ*, 686, L61
- Gill S. P. D., Knebe A., Gibson B. K., 2004, *MNRAS*, 351, 399
- Gill S. P. D., Knebe A., Gibson B. K., 2005, *MNRAS*, 356, 1327
- Gill S. P. D., Knebe A., Gibson B. K., Dopita M. A., 2004, *MNRAS*, 351, 410
- Gottlöber S., Hoffman Y., Yepes G., 2010, in S. Wagner, M. Steinmetz, A. Bode, M.M. Müller ed., *High Performance Computing in Science and Engineering Springer, Constrained Local UniversE Simulations (CLUES)*. pp 309–323
- Haardt F., Madau P., 1996, *ApJ*, 461, 20
- Hoefl M., Yepes G., Gottlöber S., Springel V., 2006, *MNRAS*, 371, 401
- Kendall M., Gibbons J. D., 1990, *Rank Correlation Methods*, 5 edn. A Charles Griffin Title
- Kennicutt Jr. R. C., 1998, in G. Gilmore & D. Howell ed., *The Stellar Initial Mass Function (38th Herstmonceux Conference)* Vol. 142 of *Astronomical Society of the Pacific Conference Series, Overview: The Initial Mass Function in Galaxies*. pp 1–+
- Klimontowski J., Łokas E. L., Knebe A., Gottlöber S., Martínez-Vaquero L. A., Yepes G., Hoffman Y., 2010, *MNRAS*, 402, 1899
- Klypin A., Kravtsov A. V., Valenzuela O., Prada F., 1999, *ApJ*, 522, 82
- Knebe A., Libeskind N. I., Knollmann S. R., Yepes G., Gottlöber S., Hoffman Y., 2010, *ArXiv e-prints*
- Knollmann S. R., Knebe A., 2009, *ApJS*, 182, 608

⁶ Note that Wadepuhl & Springel (2010) also required a shift by a factor of 5.2 for their simulation data.

- Koposov S., Belokurov V., Evans N. W., Hewett P. C., Irwin M. J., Gilmore G., Zucker D. B., Rix H., Fellhauer M., Bell E. F., Glushkova E. V., 2008, *ApJ*, 686, 279
- Li Y., Helmi A., 2008, *MNRAS*, 385, 1365
- Li Y., Helmi A., 2009, in J. Andersen, J. Bland-Hawthorn, & B. Nordström ed., *IAU Symposium Vol. 254 of IAU Symposium, Group infall of substructures on to a Milky Way-like dark halo*. pp 263–268
- Libeskind N. I., Knebe A., Hoffman Y., Gottloeber S., Yepes G., Steinmetz M., 2010, *ArXiv e-prints*
- Libeskind N. I., Yepes G., Knebe A., Gottlöber S., Hoffman Y., Knollmann S. R., 2010, *MNRAS*, 401, 1889
- Ludlow A. D., Navarro J. F., Springel V., Jenkins A., Frenk C. S., Helmi A., 2009, *ApJ*, 692, 931
- Macciò A. V., Kang X., Fontanot F., Somerville R. S., Koposov S., Monaco P., 2010, *MNRAS*, 402, 1995
- Mateo M. L., 1998, *ARA&A*, 36, 435
- Moore B., Diemand J., Stadel J., 2004, in Diaferio A., ed., *IAU Colloq. 195: Outskirts of Galaxy Clusters: Intense Life in the Suburbs On the age-radius relation and orbital history of cluster galaxies*. pp 513–518
- Moore B., Ghigna S., Governato F., Lake G., Quinn T., Stadel J., Tozzi P., 1999, *ApJ*, 524, L19
- Press W. H., Teukolsky S. A., Vetterling W. T., Flannery B. P., 1992, *Numerical recipes in C. The art of scientific computing*. Cambridge: University Press, —c1992, 2nd ed.
- Spergel et al. D. N., 2007, *ApJS*, 170, 377
- Springel V., 2005, *MNRAS*, 364, 1105
- Springel V., Hernquist L., 2003, *MNRAS*, 339, 289
- Wadepuhl M., Springel V., 2010, *ArXiv e-prints*
- Walker M. G., Mateo M., Olszewski E. W., Peñarrubia J., Wyn Evans N., Gilmore G., 2009, *ApJ*, 704, 1274
- Warnick K., Knebe A., Power C., 2008, *MNRAS*, 385, 1859

This paper has been typeset from a $\text{\TeX}/\text{\LaTeX}$ file prepared by the author.